Available online at www.sciencedirect.com

SciVerse ScienceDirect

Ceramics International 39 (2013) 5521–5525

CERAMICS INTERNATIONAL

www.elsevier.com/locate/ceramint

Luminescence properties of Br-doped ZnS nanoparticles synthesized by a low temperature solid-state reaction method

Yang Li, Sheng Zhou, Zhong Chen, Yi Yang, Nan Chen, Guoping Du*

School of Materials Science and Engineering, Nanchang University, Nanchang, Jiangxi 330031, China

Received 18 November 2012; received in revised form 19 December 2012; accepted 19 December 2012
Available online 28 December 2012

Abstract

Br-doped ZnS nanoparticles were synthesized using a low temperature solid-state reaction method. Influence of Br doping concentration on the crystal structures, crystallite sizes, and luminescence properties of the Br-doped ZnS nanoparticles was investigated. The Br-doped ZnS nanoparticles had a cubic zincblende crystal structure, and had an average crystallite size of about 8.0–9.5 nm. Both the lattice constant and average crystallite size of the Br-doped ZnS nanoparticles decreased with Br doping concentration. It was found that the luminescence intensity of the Br-doped ZnS nanoparticles remarkably increased with Br doping concentration. The emission intensity of the 5% Br-doped ZnS nanoparticles was about 13 times stronger than the undoped ZnS nanoparticles. Mechanism for the enhanced luminescence of the Br-doped ZnS nanoparticles was discussed. This work suggests that the low temperature solid-state reaction method can be used to synthesize Br-doped ZnS nanoparticles with strong luminescence properties.

Keywords: Nanoparticles; Zinc sulfide; Bromine doping; Luminescence

1. Introduction

It is well known that zinc sulfide (ZnS), a wide direct band gap semiconductor, is one of the most typical and important II–VI compound semiconductors with broad applications in different fields such as optoelectronics, catalysis, and so on [1–3]. In recent years, ZnS nanoparticles have been gaining extensive attention for their luminescence properties [4,5].

Many approaches have been employed to improve the luminescence properties of ZnS nanoparticles. It has been shown that doping can effectively enhance the luminescence properties of ZnS nanoparticles [6–18]. Elements such as Mn [6–8], Cu [9–11], Eu [12,13], Ag [14], Pb [15], Mg [16], Co [17] and Ba [18] have been doped into ZnS nanoparticles, and improved luminescence has been observed. Pathak et al. [6] used a chemical method to prepare Mn^{2+}-doped ZnS nanoparticles which were passivated by acrylic acid, and they observed enhanced luminescence after surface passivation and Mn^{2+}-related yellow emission at 574 nm at room temperature. Kuppayee et al. [9] used a co-precipitation method to synthesize Cu^{2+}-doped ZnS nanoparticles with PMMA and CTAB surfactants, and they observed a 2-fold enhancement in the luminescence after Cu^{2+} doping. In a recent work by Pathak et al. [18], they employed a simple precipitation method to synthesize Ba^{2+}-doped ZnS nanoparticles without using any capping agents, and the emission was found to be shifted from the blue region towards the visible region after Ba^{2+} doping. These reported results suggest that the luminescence properties of ZnS nanoparticles can be largely improved by doping and they can be usually synthesized by simple methods.

Although the previous studies on doped ZnS nanoparticles were mostly focused on cation doping, anions have also been found to be effective dopants for substituting S ions in ZnS nanoparticles. Shirata et al. [19] synthesized Cl-doped ZnS phosphors by firing powder mixtures of ZnS with $MgCl_2$ and NaCl at 1100 °C. Sharma et al. [20] reported the synthesis of ZnS:Cu,Cl phosphors. Corrado

*Corresponding author. Tel.: +86 791 3969553.
E-mail addresses: guopingdu@ncu.edu.cn, gpdu999@163.com (G. Du).

0272-8842/$ - see front matter © 2012 Elsevier Ltd and Techna Group S.r.l. All rights reserved.
http://dx.doi.org/10.1016/j.ceramint.2012.12.064

et al. [21] prepared Cu and Br co-doped ZnS nanocrystals with enhanced luminescence via a hot-injection method. Chander et al. [22] also prepared Cu and Br co-doped ZnS phosphors by different routes. Manzoor et al. [23] employed a wet-chemical precipitation method to synthesize ZnS nanoparticles co-doped with Cu^+ and halogen ions such as F, Cl, Br or I, and they observed a luminescence enhancement. In their work [23], the F, Cl, Br or I doping ions were supplied by ammonium halogen salts.

Different synthesis methods for ZnS nanoparticles have been reported in the literature [24]. The low temperature solid-state reaction method has been shown to be one of the simple, efficient and cost-effective methods for synthesizing ZnS nanoparticles [25–28]. Pathak et al. [26] used this method to prepare ZnS nanoparticles. Manam et al. [27] and Yu et al. [28] used this method to prepare Cu-doped and Mn-doped ZnS nanophosphors, respectively. However, synthesis of ZnS nanoparticles doped with anions using the low temperature solid-state reaction method has hardly been reported in the literature. In this work, we synthesized Br-doped ZnS nanoparticles using the low temperature solid-state reaction method, and studied their luminescence properties. A strong luminescence enhancement in the Br-doped ZnS nanoparticles was observed.

2. Experimental

Analytical-grade reagents $Zn(CH_3COO)_2$, C_2H_5NS (TAA) and NH_4Br were used without further purification. Anhydrous ethanol was used as the dissolving and washing solution, while TAA, $Zn(CH_3COO)_2$, and NH_4Br were the source materials for supplying S, Zn, and Br, respectively, for the Br-doped ZnS nanoparticles. For the undoped ZnS nanoparticles, no NH_4Br was used. All samples were synthesized using the low temperature solid-state reaction method. Br doping concentration in the Br-doped ZnS nanoparticles was set according to the molecular formulae $ZnS_{(1-x)}Br_x$, where $x=1\%$, 3%, and 5%. The reason for choosing these low doping concentrations in this work is because the differences in the ion radii and electrical charges between Br^- and S^{2-} were believed to limit the doping concentration of Br for substituting S of ZnS. However, work for higher Br doping concentrations is in progress in our group. Undoped ZnS sample (0% Br) was also synthesized for reference. First, source materials according to a desired stoichiometric ratio were weighed, and they were intimately mixed. The mixture was heated at 130 °C in an oven for 3 h. The products were washed with alcohol and deionized water, and the precipitates were retrieved by centrifugation. This procedure was repeated for several times in order to remove the residues. Finally, the precipitates were dried under vacuum at 80 °C for 1.5 h to obtain the undoped and Br-doped ZnS nanoparticles.

X-ray diffraction (XRD, Bruker D8 Focus) technique was used to study the crystal structures of the ZnS nanoparticles. The X-ray diffractometer with a graphite monochromatized Cu Kα radiation ($\lambda=0.15406$ nm) was operated at a step of 0.02° in the 2θ from 10° to 80°. Microstructural characteristics were investigated using a transmission electron microscope (TEM, JEM 2010). Luminescence properties were measured at room temperature using a Hitachi F-4600 fluorescence spectrophotometer equipped with a xenon lamp source.

3. Results and discussion

Fig. 1 shows the XRD patterns of the undoped and Br-doped ZnS nanoparticles. All the XRD peaks for these nanoparticles can be readily indexed to be the (1 1 1), (2 2 0) and (3 1 1) crystal planes of the cubic zincblende ZnS crystal structure (JCPDS card, No. 05-0566), and no impurity phases were observed. Hence, these Br-doped ZnS nanoparticles synthesized by the low temperature solid-state reaction method remained to have the cubic zincblende ZnS crystal structure. This is consistent with the results reported by others [28,29].

It is noted in Fig. 1 that the XRD peaks slightly shifted towards larger angles after Br doping, indicating a smaller lattice constant for the Br-doped ZnS nanoparticles. The lattice constant a can be calculated using the Bragg equation [30]:

$$a=\frac{\lambda}{2\sin\theta}\sqrt{h^2+k^2+l^2} \quad (1)$$

where λ is the X-ray wavelength (1.54056 Å), θ is the Bragg angle, and (hkl) is the Miller index of crystal plane. The calculated lattice constant was 5.3861 Å for the undoped ZnS nanoparticles, and 5.3817 Å, 5.3687 Å and 5.3579 Å for the Br-doped ZnS nanoparticles with Br doping

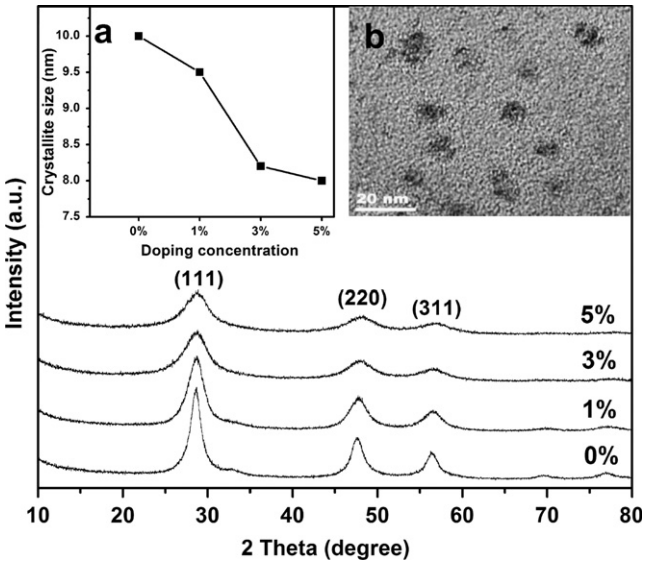

Fig. 1. XRD patterns of the undoped and Br-doped (1%, 3%, 5%) ZnS nanoparticles. Inset a shows the variation of the calculated crystallite size with Br doping concentration, and inset b shows the TEM image of the 5% Br-doped ZnS nanoparticles.

concentrations of 1%, 3% and 5% in order. Nevertheless, it is known [31] that Br (182 pm) has a larger ionic radius than S (170 pm). Thus, a larger lattice constant would be expected for the Br-doped ZnS nanoparticles. With regard to the reason for such a decrease of lattice constant with Br doping concentration for the Br-doped ZnS nanoparticles, we suppose that the generation of Zn vacancies should be the cause. Br^- and S^{2-} have different electrical charges, so every two substituting Br ions can generate an extra Zn vacancy due to the requirement of electrical charge neutrality within the ZnS host lattice. The generation of extra Zn vacancies resulted in a contraction of lattice constant for the Br-doped ZnS in spite of the larger ionic radius for Br than *S*.

As shown in Fig. 1, these XRD peaks became broader with the increase of Br doping concentration. The average crystallite size of nanoparticles can be calculated from the XRD patterns using the Debye–Scherrer equation [32]:

$$d = 0.89\lambda/\beta \cos\theta \quad (2)$$

where d is the crystallite size, λ is the X-ray wavelength, β is the full width at half maximum of a XRD peak, and θ is the Bragg angle. The calculated average crystallite sizes of the undoped ZnS and Br-doped nanoparticles were shown in Fig. 1 (inset a). The crystallite size decreased from about 10 nm for the undoped ZnS nanoparticles to around 9.5, 8.2 and 8.0 nm for the Br-doped ZnS nanoparticles with Br doping concentrations of 1%, 3% and 5%, respectively. The inset b of Fig. 1 shows the TEM image of the 5% Br-doped ZnS nanoparticles, and the crystallite size was about 8–9 nm, which is approximately in agreement with the calculated (Eq. (2)) crystallite sizes (Fig. 1 inset a) based on the XRD pattern. This is also consistent with the results reported by others [28] for the Mn-doped ZnS nanoparticles synthesized by the low temperature solid-state reaction method.

It is noted in Fig. 1 that the XRD peaks of these Br-doped ZnS nanoparticles became weaker with the increase of Br doping concentration. This suggests that the crystallinity of ZnS nanoparticles decreased with Br doping concentration. Two sources of contribution are responsible for this behavior [16]. One is the distortion in the ZnS host lattice caused by the Br dopants. Another source is the generation of Zn vacancies in the ZnS host lattice as stated in the previous paragraphs.

To further investigate the composition and chemical state of these samples, we used the X-ray photoelectron spectroscopy (XPS) to characterize the undoped and 5% Br-doped ZnS nanoparticles. Their XPS spectra are shown in Fig. 2. XPS peaks of Zn, S, C and O are observed in Fig. 2a, where the presence of C and O was due to the sample holder and surface absorption of oxygen when exposed in air. The inset of Fig. 2a clearly shows the presence of Br dopants for the 5% Br-doped ZnS nanoparticles [33]. However, no trace of Br was detected in the undoped ZnS nanoparticles (Fig. 2a inset). It can be seen in Fig. 2b that the binding energy of the Zn 2p electrons became higher after Br doping. This suggests that Br ions effectively doped into the ZnS lattice and chemically interacted with Zn ions.

The excitation and emission spectra of the undoped and Br-doped ZnS nanoparticles are shown in Fig. 3. Two excitation bands in the UV range with their maxima at about 277 nm and 322 nm can be clearly seen in Fig. 3a. The first excitation band peaking at about 277 nm corresponded to a band gap of 4.48 eV, which was related to the band to band transition of electrons. As shown by the schematic energy-level diagram in Fig. 4 [34–36], the second excitation band peaking at about 322 nm (3.85 eV) is believed to be a result of the combined effect from (1) the transition of electrons from valence band to the donor levels such as sulfur vacancy (V_S) and bromine defects ($Br_S^{\bullet}$), and (2) the transition of electrons from the Zn vacancy-related acceptor levels such as, V''_{Zn}, $(V_{Zn}Br)'$ and V'_{Zn}, to the conduction band. It is noted in Fig. 3a that the excitation intensity quickly increased with Br doping concentration. This suggests that Br doping had a strong effect in improving the luminescence properties of ZnS nanoparticles. For the undoped and 1% Br-doped ZnS nanoparticles, the excitation band peaking at about 277 nm was relatively stronger than the one peaking at 322 nm (Fig. 3a). However, the 3% and 5% Br-doped ZnS

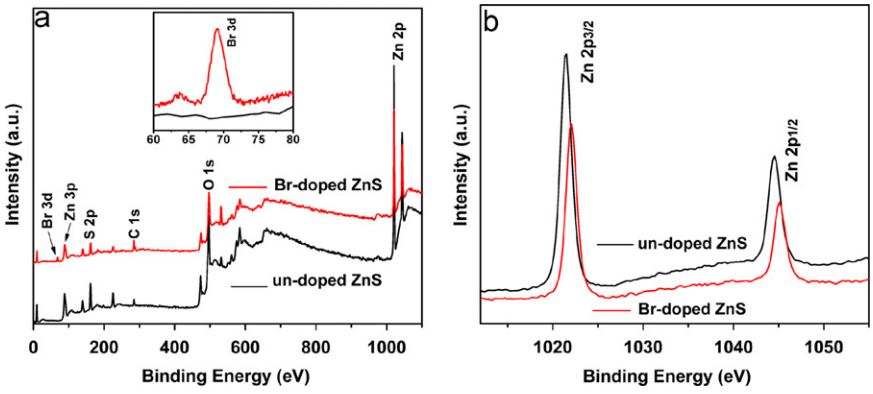

Fig. 2. XPS spectra of the undoped and 5% Br-doped ZnS nanoparticles: (a) the full spectra with an inset showing the presence and absence of Br in the Br-doped and undoped samples, (b) the chemical shift for the Zn 2p electrons after Br doping.

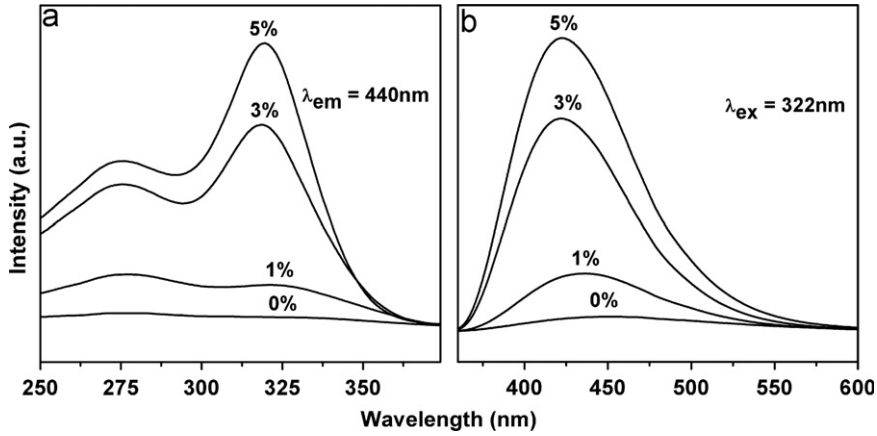

Fig. 3. Luminescence spectra of the undoped and Br-doped ZnS nanoparticles for excitation (a) and emission (b).

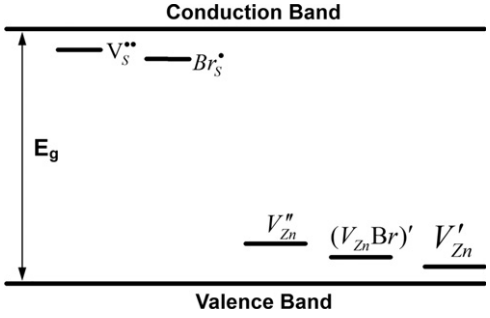

Fig. 4. Schematic energy-level diagram for the Br-doped ZnS nanoparticles.

nanoparticles exhibited quite different behavior as shown in Fig. 3a, where one can see that their excitation band peaking at about 322 nm was much stronger than the one peaking at 277 nm. In fact, this result supports the point that the excitation band peaking at about 322 nm was from the Zn vacancy-related acceptor levels as stated earlier in this paragraph. Higher Br doping concentration led to a larger number of Zn vacancies in the ZnS host lattice, and a luminescence enhancement is therefore expected for the ZnS nanoparticles.

As shown in Fig. 3b, a single emission band was observed for each of these samples, and it peaked at about 421–440 nm. Similar to the excitation spectra (Fig. 3a), the emission intensity remarkably increased with Br doping concentration (Fig. 3b). The emission intensity of the 5% Br-doped ZnS nanoparticles was about 13 times stronger than the undoped ZnS nanoparticles. Moreover, a blue shift in the emission peak can be clearly observed for the Br-doped ZnS nanoparticles as shown in Fig. 3b. This can be attributed to the quantum size effect [37,38] caused by the decrease of ZnS nanoparticle size as shown in Fig. 1 (inset a). When Br substitutes for S in the ZnS lattice, in addition to the generation of extra Zn vacancies, a donor-like Br_S is formed. More importantly, the Zn vacancies and donor-like Br_S can easily form a large number of zinc vacancy–bromine complexes $(V_{Zn}Br)'$. Due to the smaller energy difference between the donor–acceptor pairs as shown in Fig. 4 than the band gap, a higher chance of radiative recombination from the donor–acceptor pairs is resulted. Hence, a stronger emission is resulted in the Br-doped ZnS nanoparticles.

4. Conclusions

In summary, we successfully synthesized Br-doped ZnS nanoparticles with different Br doping concentrations using the low temperature solid-state reaction method. The influence of Br doping concentration on the crystal structures, crystallite sizes, and luminescence properties of the Br-doped ZnS nanoparticles was investigated. The Br-doped ZnS nanoparticles had a cubic zincblende crystal structure, and their average crystallite sizes was about 8.0–9.5 nm. Both the lattice constant and the average crystallite size of the Br-doped ZnS nanoparticles were found to decrease with Br doping concentration. The reducing lattice constant with Br doping was a result of the generation of Zn vacancies. The luminescence intensity of the Br-doped ZnS nanoparticles remarkably increased with Br doping concentration. The 5% Br-doped ZnS nanoparticles was found to have an emission intensity about 13 times stronger than the undoped ZnS nanoparticles. The enhanced luminescence of the Br-doped ZnS nanoparticles was a result of radiative recombination from the defect related donor–acceptor pairs. This work indicates that Br-doped ZnS nanoparticles with strong luminescence properties can be synthesized using the facile low temperature solid-state reaction method.

Acknowledgments

This work was supported by the National Natural Science Foundation of China (60661001) and the Program for Innovative Research Team of Nanchang University.

References

[1] T. Ohno, K. Kurisu, T. Taguchi, Growth of high-quality cubic ZnS crystals and their application to MIS blue light-emitting-diodes, Journal of Crystal Growth 99 (1990) 737–742.

[2] P.I. Ekwo, C.E. Okeke, Thermoelectric properties of the PbS-ZnS alloy semiconductor and its application to solar-energy conversion, Energy Conversion and Management 33 (1992) 159–164.
[3] L.P. Colletti, R. Slaughter, J.L. Stickney, Electrochemical formation of ZnS screens, Journal of the Society for Information Display 5 (1997) 87–92.
[4] N. Karar, H. Chander, Nanocrystal formation and luminescence properties of ZnS based doped nanophosphors, Journal of Nanoscience Nanotechnology 5 (2005) 1498–1502.
[5] C.L. Lu, J.F. Gao, Y.Q. Fu, Y.Y. Du, Y.L. Shi, Z.M. Su, A ligand exchange route to highly luminescent surface-functionalized ZnS nanoparticles and their transparent polymer nanocomposites, Advanced Functional Materials 18 (2008) 3070–3079.
[6] C.S. Pathak, M.K. Mandal, Enhanced photoluminence properties of Mn^{2+} doped ZnS nanoparticles, Chalcogenide Letters 8 (2011) 147–153.
[7] R.N. Bhargava, D. Gallagher, X. Hong, A. Nurmikko, Optical-properties of manganese-doped nanocrystals of ZnS, Physical Review Letters 72 (1994) 416–419.
[8] H. Yang, Z.C. Wang, L.Z. Song, M.Y. Zhao, Y.M. Chen, K. Dou, J.Q. Yu, L. Wang, Study of optical properties of manganese doped ZnS nanocrystals, Materials Chemistry and Physics 47 (1997) 249–251.
[9] M. Kuppayee, G.K.V. Nachiyar, V. Ramasamy, Enhanced photoluminescence properties of ZnS:Cu^{2+} nanoparticles using PMMA and CTAB surfactants, Materials Science in Semiconductor Processing 15 (2012) 136–144.
[10] J.M. Huang, Y. Yang, S.H. Xue, B. Yang, S.Y. Liu, J.C. Shen, Photoluminescence and electroluminescence of ZnS:Cu nanocrystals in polymeric networks, Applied Physics Letters 70 (1997) 2335–2337.
[11] L.D. Sun, C.H. Liu, C.S. Liao, C.H. Yan, ZnS nanoparticles doped with Cu(I) by controlling coordination and precipitation in aqueous solution, Journal of Materials Chemistry 9 (1999) 1655–1657.
[12] W. Chen, J.O. Malm, V. Zwiller, Y.N. Huang, S.M. Liu, R. Wallenberg, J.O. Bovin, L. Samuelson, Energy structure and fluorescence of Eu^{2+} in ZnS:Eu nanoparticles, Physical Review B 61 (2000) 11021–11024.
[13] S.C. Qu, W.H. Zhou, F.Q. Liu, N.F. Chen, Z.G. Wang, H.Y. Pan, D.P. Yu, Photoluminescence properties of Eu^{3+}-doped ZnS nanocrystals prepared in a water/methanol solution, Applied Physics Letters 80 (2002) 3605–3607.
[14] W.P. Jian, J.Q. Zhuang, D.W. Zhang, J. Dai, W.S. Yang, Y.B. Bai, Synthesis of highly luminescent and photostable ZnS:Ag nanocrystals under microwave irradiation, Materials Chemistry and Physics 99 (2006) 494–497.
[15] P.H. Borse, W. Vogel, S.K. Kulkarni, Effect of pH on photoluminescence enhancement in Pb-doped ZnS nanoparticles, Journal of Colloid and Interface Science 293 (2006) 437–442.
[16] Z. Chen, X.X. Li, N. Chen, G.P. Du, Y.S. Li, G.H. Liu, A.Y.M. Suen, Study on the optical properties of $Zn_{1-x}Mg_xS$ ($0 \le x \le 0.55$) quantum dots prepared by precipitation method, Materials Science and Engineering B 177 (2012) 337–340.
[17] C. Vatankhah, M.H. Yuosefi, A.A. Khosravi, M. Savarian, The study of optical properties of ZnS, ZnS:Co2+ nanoparticles, European Physical Journal – Applied Physics 48 (2009) 20601 (3 pages)..
[18] C.S. Pathak, D.D. Mishra, V. Agarwala, M.K. Mandal, Blue light emission from barium doped zinc sulfide nanoparticles, Ceramics International 38 (2012) 5497–5500.
[19] M. Shirata, K. Shimizu, T. Koike, T. Komiyama, T. Matsui, Y. Nakanishi, K. Hara, Effect of Ir^{3+} Incorporation on the Luminescent Properties of ZnS:Cl Phosphors, Journal of the Electrochemical Society 158 (2011) H318–H321.
[20] G. Sharma, S.D. Han, J.D. Kim, S.P. Khatkar, Y.W. Rhee, Electroluminescent efficiency of alternating current thick film devices using ZnS: Cu,Cl phosphor, Materials Science & Engineering B 131 (2006) 271–276.
[21] C. Corrado, J.K. Cooper, M. Hawker, J. Hensel, G. Livingston, S. Gul, B. Vollbrecht, F. Bridges, J.Z. Zhang, Synthesis and characterization of organically soluble Cu-doped ZnS nanocrystals with Br Co-activator, Journal of Physical Chemistry C 115 (2011) 14559–14570.
[22] H. Chander, V. Shanker, D. Haranath, S. Dudeja, P. Sharma, Characterization of ZnS:Cu, Br electroluminescent phosphor prepared by new route, Materials Research Bulletin 38 (2003) 279–288.
[23] K. Manzoor, S.R. Vadera, N. Kumar, T.R.N. Kutty, Synthesis and photoluminescent properties of ZnS nanocrystals doped with copper and halogen, Materials Chemistry and Physics 82 (2003) 718–725.
[24] X. Fang, T. Zhai, U.K. Gautam, L. Li, L. Wu, Y. Bando, D. Golberg, ZnS nanostructures: from synthesis to applications, Progress in Materials Science 56 (2011) 175–287.
[25] L.P. Wang, G.Y. Hong, A new preparation of zinc sulfide nanoparticles by solid-state method at low temperature, Materials Research Bulletin 35 (2000) 695–701.
[26] C.S. Pathak, D.D. Mishra, V. Agarwala, M.K. Mandal, Optical properties of ZnS nanoparticles produced by mechanochemical method, Ceramics International 38 (2012) 6191–6195.
[27] J. Manam, V. Chatterjee, S. Das, A. Choubey, S.K. Sharma, Preparation, characterization and study of optical properties of ZnS nanophosphor, Journal of Luminescence 130 (2010) 292–297.
[28] G. Murugadoss, Luminescence properties of co-doped ZnS:Ni, Mn and ZnS:Cu, Cd nanoparticles, Journal of Luminescence 132 (2012) 2043–2048.
[29] X. Bin, I.W. Lenggoro, K. Okuyama, Synthesis and photoluminescence of spherical ZnS:Mn2+ particles, Chemistry of Materials 14 (2002) 4969–4974.
[30] W.L. Bond, Precision lattice constant determination, Acta Crystallographica 13 (1960) 814–818.
[31] R.D. Shannon, Revised effective ionic radii and systematic studies of interatomic distances in halides and chalcogenides, Acta Crystallographica A 32 (1976) 751–767.
[32] E.F. Kaelble, Handbook of X-Rays, McGraw-Hill, New York, 1967.
[33] J.F. Moulder, W.F. Stickle, P.E. Sobol, K.D. Bomben, Handbook of X-Ray Photoelectron Spectroscopy, 1st ed., Perkin-Elmer Corporation, Minnesota, 1979.
[34] A.N. Georgobiani, R.G. Maev, Y.V. Ozerov, E.E. Strumban, Investigation of deep centres of chlorine-doped zinc sulfide crystals, Physica Status Solidi A 38 (1976) 77–83.
[35] J.S. Lewis, M.R. Davidson, P.H. Holloway, Control of point defects and space charge in electroluminescent ZnS:Mn thin films, Journal of Applied Physics 92 (2002) 6646–6657.
[36] H. Samelson, A. Lempicki, Fluorescence of cubic ZnS:Cl crystals, Physical Review 125 (1962) 901–909.
[37] T. Takagahara, K. Takeda, Theory of the quantum confinement effect on excitons in quantum dots of indirect-gap materials, Physical Review B 46 (1992) 15578–15581.
[38] N. Chestnoy, T.D. Harris, R. Hull, L.E. Brus, Luminescence and photophysics of cadmium sulfide semiconductor clusters: the nature of the emitting electronic state, Journal of Physical Chemistry 90 (1986) 3393–3399.